

SOFT MIXTURE DENOISING: BEYOND THE EXPRESSIVE BOTTLENECK OF DIFFUSION MODELS

Yangming Li, Boris van Breugel, Mihaela van der Schaar

Department of Applied Mathematics and Theoretical Physics

University of Cambridge

{y1874, bv292, mv472}@cam.ac.uk

ABSTRACT

Because diffusion models have shown impressive performances in a number of tasks, such as image synthesis, there is a trend in recent works to prove (with certain assumptions) that these models have strong approximation capabilities. In this paper, we show that current diffusion models actually have an *expressive bottleneck* in backward denoising and some assumption made by existing theoretical guarantees is too strong. Based on this finding, we prove that diffusion models have unbounded errors in both local denoising and global approximation. In light of our theoretical studies, we introduce *soft mixture denoising* (SMD), an expressive and efficient model for backward denoising. SMD not only permits diffusion models to well approximate any Gaussian mixture distributions in theory, but also is simple and efficient for implementation. Our experiments on multiple image datasets show that SMD significantly improves different types of diffusion models (e.g., DDPM), especially in the situation of few backward iterations.

1 INTRODUCTION

Diffusion models (Sohl-Dickstein et al., 2015) have become highly popular generative models for their impressive performances in many research domains. For example, high-resolution image synthesis (Dhariwal & Nichol, 2021), natural language generation (Li et al., 2022), speech processing (Kong et al., 2021), and medical image analysis (Pinaya et al., 2022).

Current strong approximator theorems. To explain the effectiveness of diffusion models, some recent works (Lee et al., 2022a;b; Chen et al., 2023) provided theoretical guarantees (with certain assumptions) to show that diffusion models can approximate a rich family of data distributions with arbitrarily small errors. For example, Chen et al. (2023) proved that the generated samples from diffusion models converge (in distribution) to the real data under ideal conditions. Because it is generally intractable to analyze the non-convex optimization of neural networks, a potential weakness of these works is that they all supposed *perfect score functions*, which means the prediction errors of denoising functions (i.e., reparameterized score functions) are bounded.

Our limited approximation theorems. In this work, we take a first step towards the opposite direction of prior works. Instead of explaining why diffusion models are highly effective, we show that their approximation capabilities are in fact limited and the assumption of *perfect score functions* is too strong, which both challenge the current theoretical guarantees.

An informal overview of our theoretical studies: we first show an **expressive bottleneck** of current diffusion models — The Gaussian form of backward probability $p_\theta(\mathbf{x}_{t-1} | \mathbf{x}_t)$ is not expressive enough to fit potentially very complex posterior probability $q(\mathbf{x}_{t-1} | \mathbf{x}_t)$. With this finding, we then prove that *diffusion models will have arbitrarily large denoising errors for approximating some common data distribution $q(\mathbf{x}_0)$ (e.g., Gaussian mixture)*, indicating that the assumption of perfect score functions made by previous theoretical guarantees is too strong. Lastly and importantly, we prove that *diffusion models will have an arbitrarily large error in matching the learnable backward process $p_\theta(\mathbf{x}_{0:T})$ with the predefined forward process $q(\mathbf{x}_{0:T})$* , which is actually the optimization objective of current diffusion models (Ho et al., 2020; Song et al., 2021b). This fact indicates that these models will fail to approximate some complex data distribution $q(\mathbf{x}_0)$.

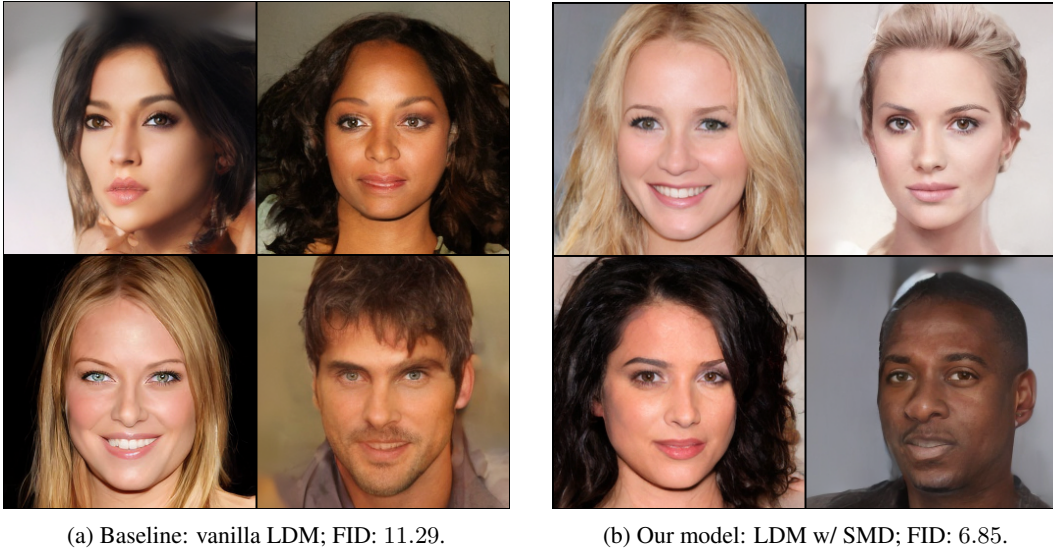


Figure 1: The baseline and our model are both trained on CelebA-HQ 256×256 with only 100 backward iterations. The FID score of LDM (Rombach et al., 2022) with 1000 iterations is around 6. Our model performs close to that with much fewer backward iterations. Note that our proposed SMD differs from the current fast samplers, such as DDIM (Song et al., 2021a) and DPM (Lu et al., 2022). *While those methods focus on deterministic sampling and numerical stability, SMD aims to improve the expressiveness of diffusion models.*

Our method: soft mixture denoising (SMD). In light of our theoretical findings, we propose an expressive and efficient backward denoising model $p_{\theta}^{\text{SMD}}(\mathbf{x}_{t-1} | \mathbf{x}_t)$, soft mixture denoising (SMD), which represents the hidden mixture components of posterior probability $q(\mathbf{x}_{t-1} | \mathbf{x}_t)$ with a continuous latent variable \mathbf{z}_t . SMD not only has a solid theoretical foundation but also is simple and efficient to implement. For the former, we prove that *SMD permits diffusion models to well approximate any Gaussian mixture distributions*. For the latter, we reparameterize our model and derive an upper bound of the negative log-likelihood for optimization.

We have conducted extensive experiments on multiple image datasets, showing that SMD significantly improves different types of diffusion models (e.g., DDPM (Ho et al., 2020) and LDM (Rombach et al., 2022)). Plus, we show that SMD improves DDPM the most for few backward iterations. A preview of that experiment is in Fig. 1. With SMD, we no longer have to configure the diffusion model with 1000 backward iterations: $T = 1000$.

Contributions. In summary, our contributions are threefold:

1. In terms of theoretical studies, we find that current diffusion models suffer from an *expressive bottleneck* and prove that the models have unbounded errors in both local denoising and global approximation. Our theorems also indicate that the assumption of *perfect score functions* made by current theoretical guarantees is too strong;
2. In terms of methodology, we introduce SMD, an expressive backward denoising model. Not only SMD permits the diffusion models to well fit very complex data distributions, but also it is simple and efficient for implementation;
3. In terms of experiments, we show that SMD significantly improves different types of diffusion models, especially in the case of few backward iterations. With SMD, we no longer have to configure the diffusion models with 1000 backward iterations.

We will publicly release our code at <https://XXX> once the paper is accepted.

2 BACKGROUND: DISCRETE-TIME DIFFUSION MODELS

In this section, we briefly review the mainstream architecture of diffusion models in discrete time (e.g., DDPM (Ho et al., 2020)). The notations and terminologies introduced below are necessary preparations for diving into our subsequent sections.

A diffusion model typically consists of two Markov chains of T steps. One of them is the forward process — also known as the diffusion process — which incrementally adds Gaussian noises to the real sample $\mathbf{x}_0 \in \mathbb{R}^D$, $D \in \mathbb{N}$, giving a chain of variables $\mathbf{x}_{1:T} = [\mathbf{x}_1, \mathbf{x}_2, \dots, \mathbf{x}_T]$:

$$q(\mathbf{x}_{1:T} | \mathbf{x}_0) = \prod_{t=1}^T q(\mathbf{x}_t | \mathbf{x}_{t-1}), \quad q(\mathbf{x}_t | \mathbf{x}_{t-1}) = \mathcal{N}(\mathbf{x}_t; \sqrt{1 - \beta_t} \mathbf{x}_{t-1}, \beta_t \mathbf{I}), \quad (1)$$

where \mathcal{N} denotes a Gaussian distribution, \mathbf{I} represents an identity matrix, and $\beta_t, 1 \leq t \leq T$ are a predefined variance schedule. By properly defining the variance schedule, the last variable \mathbf{x}_T will approximately follow a normal Gaussian distribution.

The second part of diffusion models is the *backward* (or *reverse*) *process*. Specifically speaking, the process first draws an initial sample \mathbf{x}_T from a standard Gaussian $p(\mathbf{x}_T) = \mathcal{N}(\mathbf{0}, \mathbf{I})$ and then gradually denoises it into a sequence of variables $\mathbf{x}_{T-1:0} = [\mathbf{x}_{T-1}, \mathbf{x}_{T-2}, \dots, \mathbf{x}_0]$:

$$p_\theta(\mathbf{x}_{T:0}) = p(\mathbf{x}_T) \prod_{t=T}^1 p_\theta(\mathbf{x}_{t-1} | \mathbf{x}_t), \quad p_\theta(\mathbf{x}_{t-1} | \mathbf{x}_t) = \mathcal{N}(\mathbf{x}_{t-1}; \boldsymbol{\mu}_\theta(\mathbf{x}_t, t), \sigma_t \mathbf{I}), \quad (2)$$

where $\sigma_t \mathbf{I}$ is a predefined covariance matrix and $\boldsymbol{\mu}_\theta$ is a learnable module with the parameter θ to predict the mean vector. Most ideally, the learnable backward probability $p_\theta(\mathbf{x}_{t-1} | \mathbf{x}_t)$ is equal to the inverse forward probability $q(\mathbf{x}_{t-1} | \mathbf{x}_t)$ at every iteration $t \in [1, T]$ such that the backward process is just a reverse version of the forward process.

Since the exact negative log-likelihood $\mathbb{E}[-\log p_\theta(\mathbf{x}_0)]$ is computationally intractable, common practices adopt its upper bound \mathcal{L} as the loss function:

$$\begin{aligned} \mathbb{E}_{\mathbf{x}_0 \sim q(\mathbf{x}_0)}[-\log p_\theta(\mathbf{x}_0)] &\leq \underbrace{\mathbb{E}_q[\mathcal{D}_{\text{KL}}[q(\mathbf{x}_T | \mathbf{x}_0), p(\mathbf{x}_T)]]}_{\mathcal{L}_T} + \underbrace{\mathbb{E}_q[-\log p_\theta(\mathbf{x}_0 | \mathbf{x}_1)]}_{\mathcal{L}_0} \\ &+ \sum_{1 < t \leq T} \underbrace{\mathbb{E}_q[\mathcal{D}_{\text{KL}}[q(\mathbf{x}_{t-1} | \mathbf{x}_t, \mathbf{x}_0), p_\theta(\mathbf{x}_{t-1} | \mathbf{x}_t)]]}_{\mathcal{L}_{t-1}} = \mathcal{L}, \end{aligned} \quad (3)$$

where \mathcal{D}_{KL} denotes the KL divergence. Every term of this loss has an analytic form so that it is computationally optimizable. Ho et al. (2020) further applied some reparameterization tricks to the loss \mathcal{L} for reducing its variance. As a result, the module $\boldsymbol{\mu}_\theta$ is reparameterized as:

$$\boldsymbol{\mu}_\theta(\mathbf{x}_t, t) = \frac{1}{\sqrt{\alpha_t}} \left(\mathbf{x}_t - \frac{\beta_t}{\sqrt{1 - \bar{\alpha}_t}} \boldsymbol{\epsilon}_\theta(\mathbf{x}_t, t) \right), \quad (4)$$

where $\alpha_t = 1 - \beta_t$, $\bar{\alpha}_t = \prod_{t'=1}^t \alpha_{t'}$, and $\boldsymbol{\epsilon}_\theta$ is parameterized by neural networks. Under this popular scheme, the loss \mathcal{L} is finally simplified as

$$\mathcal{L} = \sum_{t=1}^T \mathbb{E}_{\mathbf{x}_0 \sim q(\mathbf{x}_0), \boldsymbol{\epsilon} \sim \mathcal{N}(\mathbf{0}, \mathbf{I})} \left[\|\boldsymbol{\epsilon} - \boldsymbol{\epsilon}_\theta(\sqrt{\bar{\alpha}_t} \mathbf{x}_0 + \sqrt{1 - \bar{\alpha}_t} \boldsymbol{\epsilon}, t)\|^2 \right], \quad (5)$$

where the denoising function $\boldsymbol{\epsilon}_\theta$ is tasked to fit Gaussian noise $\boldsymbol{\epsilon}$.

3 THEORETICAL STUDIES: EXPRESSIVE BOTTLENECK

In this section, we first show that the Gaussian denoising paradigm leads to an *expressive bottleneck* for diffusion models to fit some complex data distribution $q(\mathbf{x}_0)$. Then, we properly define two errors $\mathcal{M}_t, \mathcal{E}$ that measure the approximation capability of general diffusion models and prove that they are both unbounded in terms of the current models.

3.1 LIMITED GAUSSIAN DENOISING

The core of diffusion models is to let the learnable backward probability $p_\theta(\mathbf{x}_{t-1} | \mathbf{x}_t)$ at every iteration t fit the posterior forward probability $q(\mathbf{x}_{t-1} | \mathbf{x}_t)$. From Eq. (2), we can see that the learnable probability is configured as a simple Gaussian $\mathcal{N}(\mathbf{x}_{t-1}; \boldsymbol{\mu}_\theta(\mathbf{x}_t, t), \sigma_t \mathbf{I})$. While this setup is analytically tractable and computationally efficient, our proposition below shows that its approximation goal $q(\mathbf{x}_{t-1} | \mathbf{x}_t)$ might be much more complex.

Proposition 3.1 (Non-Gaussian Inverse Probability). *For the diffusion process defined in Eq. (1), if real data \mathbf{x}_0 follow a mixture of Gaussians, then the posterior forward probability $q(\mathbf{x}_{t-1} | \mathbf{x}_t)$ at every iteration $t \in [1, T]$ is another Gaussian mixture.*

Remark 3.1. The Gaussian mixture in theory is a universal approximator of smooth probability densities (Dalal & Hall, 1983; Goodfellow et al., 2016). Therefore, this proposition implies that the posterior forward probability $q(\mathbf{x}_{t-1} | \mathbf{x}_t)$ can be arbitrarily complex.

Proof. The proof to this proposition is fully provided in the appendix. An overview is as follows. Suppose the distribution of real data $q(\mathbf{x}_0)$ is as $\sum_{k=1}^K w_k \mathcal{N}(\mathbf{x}_0; \boldsymbol{\mu}_k, \boldsymbol{\Sigma}_k)$, which consists of K multivariate Gaussians with mixture weight w_k , mean vector $\boldsymbol{\mu}_k$, and covariance matrix $\boldsymbol{\Sigma}_k$, then each posterior probability $q(\mathbf{x}_{t-1} | \mathbf{x}_t), t \in [1, T]$ has a closed-form solution:

$$q(\mathbf{x}_{t-1} | \mathbf{x}_t) = \sum_{k=1}^K w'_k \mathcal{N}(\mathbf{x}_{t-1}; \boldsymbol{\mu}'_k, \boldsymbol{\Sigma}'_k), \quad (6)$$

where mixture coefficient w'_k , mean vector $\boldsymbol{\mu}'_k$, and covariance matrix $\boldsymbol{\Sigma}'_k, 1 \leq k' \leq K$ for every Gaussian component is formulated as

$$\begin{cases} w'_k = \frac{w_k}{q(\mathbf{x}_t)} \mathcal{N}(\mathbf{x}_t; \sqrt{\bar{\alpha}_t} \boldsymbol{\mu}_k, (1 - \bar{\alpha}_t) \mathbf{I} + \bar{\alpha}_t \boldsymbol{\Sigma}_k) \\ \boldsymbol{\mu}'_k = (\mathbf{I} + \boldsymbol{\Lambda}_k^{-1})^{-1} \frac{\mathbf{x}_t}{\sqrt{\alpha_t}} + (\mathbf{I} + \boldsymbol{\Lambda}_k)^{-1} \sqrt{\bar{\alpha}_{t-1}} \boldsymbol{\mu}_k, \\ \boldsymbol{\Sigma}'_k = \frac{1 - \alpha_t}{\alpha_t} (\mathbf{I} + \boldsymbol{\Lambda}_k^{-1})^{-1} \end{cases} \quad (7)$$

where matrix $\boldsymbol{\Lambda}_k$ is defined as $(\alpha_t - \bar{\alpha}_t)/(1 - \alpha_t) \mathbf{I} + \bar{\alpha}_t/(1 - \alpha_t) \boldsymbol{\Sigma}_k$. From these two equations, we can see that inverse probability $q(\mathbf{x}_{t-1} | \mathbf{x}_t)$ is also a Gaussian mixture. \square

While diffusion models perform well in practice, we can infer from above that the Gaussian denoising paradigm $p_\theta(\mathbf{x}_{t-1} | \mathbf{x}_t) = \mathcal{N}(\mathbf{x}_{t-1}; \boldsymbol{\mu}_\theta(\mathbf{x}_t, t), \sigma_t \mathbf{I})$ in fact causes a bottleneck for the backward probability to fit the potentially multimodal distribution $q(\mathbf{x}_{t-1} | \mathbf{x}_t)$. Plus, this problem is certainly not rare since real-world data distribution $q(\mathbf{x}_0)$ is commonly non-Gaussian.

Takeaway: The posterior forward probability $q(\mathbf{x}_{t-1} | \mathbf{x}_t)$ can be an arbitrarily complex distribution for the learnable backward probability $p_\theta(\mathbf{x}_{t-1} | \mathbf{x}_t)$ — a simple Gaussian — to fit. We call this problem the *expressive bottleneck* of diffusion models.

3.2 DENOISING AND APPROXIMATION ERRORS

To quantify the impact of *expressive bottleneck* on diffusion models, we define two error measures in terms of local denoising and global approximation (i.e., the discrepancy between forward process $q(\mathbf{x}_{0:T})$ and backward process $p_\theta(\mathbf{x}_{0:T})$).

Derivation of the local denoising error. Considering the form of loss term \mathcal{L}_{t-1} in Eq. (3), we apply the KL divergence to estimate the approximation error of every learnable backward probability $p_\theta(\mathbf{x}_{t-1} | \mathbf{x}_t), t \in [1, T]$ to its reference $q(\mathbf{x}_{t-1} | \mathbf{x}_t)$ as $\mathcal{D}_{\text{KL}}[q(\mathbf{x}_{t-1} | \mathbf{x}_t), p_\theta(\mathbf{x}_{t-1} | \mathbf{x}_t)]$. Since the error depends on variable \mathbf{x}_t , we normalize it with density $q(\mathbf{x}_t)$ into $\mathbb{E}[\mathcal{D}_{\text{KL}}[\cdot]] = \int_{\mathbf{x}_t} q(\mathbf{x}_t) \mathcal{D}_{\text{KL}}[\cdot] d\mathbf{x}_t$. Importantly, we take the infimum of this error over the parameter space Θ as $\inf_{\theta \in \Theta} (\int_{\mathbf{x}_t} q(\mathbf{x}_t) \mathcal{D}_{\text{KL}}[q(\cdot), p_\theta(\cdot)] d\mathbf{x}_t)$, which means neural networks are globally optimized. In light of the above derivation, we have the following definition.

Definition 3.1 (Local Denoising Error). For every learnable backward probability $p_\theta(\mathbf{x}_{t-1} | \mathbf{x}_t)$, $1 \leq t \leq T$ in a diffusion model, its error of best approximation (i.e., parameter θ is globally optimized) to the reference $q(\mathbf{x}_{t-1} | \mathbf{x}_t)$ is defined as

$$\begin{aligned} \mathcal{M}_t &= \inf_{\theta \in \Theta} \left(\mathbb{E}_{\mathbf{x}_t \sim q(\mathbf{x}_t)} [\mathcal{D}_{\text{KL}}[q(\mathbf{x}_{t-1} | \mathbf{x}_t), p_\theta(\mathbf{x}_{t-1} | \mathbf{x}_t)]] \right) \\ &= \inf_{\theta \in \Theta} \left(\int_{\mathbf{x}_t} \underbrace{q(\mathbf{x}_t)}_{\text{Density Weight}} \underbrace{\mathcal{D}_{\text{KL}}[q(\mathbf{x}_{t-1} | \mathbf{x}_t), p_\theta(\mathbf{x}_{t-1} | \mathbf{x}_t)]}_{\text{Denoising Error w.r.t. the Input } \mathbf{x}_t} d\mathbf{x}_t \right), \end{aligned} \quad (8)$$

where space Θ represents the set of all possible parameters. Note that the inequality $\mathcal{M}_t \geq 0$ always holds because KL divergence is non-negative.

Significance of the global approximation error. Current practices (Ho et al., 2020) expect the backward process $p_\theta(\mathbf{x}_{0:T})$ to exactly match the forward process $q(\mathbf{x}_{0:T})$ such that their marginals at iteration 0 are equal: $q(\mathbf{x}_0) = p_\theta(\mathbf{x}_0)$. For example, Song et al. (2021b) directly configured the backward process as the reverse-time diffusion equation. Hence, we have the following error definition to measure the global approximation capability of diffusion models.

Definition 3.2 (Global Approximation Error). The discrepancy between learnable backward process $p_\theta(\mathbf{x}_{0:T})$ and predefined forward process $q(\mathbf{x}_{0:T})$ is estimated as

$$\mathcal{E} = \inf_{\theta \in \Theta} \left(\mathcal{D}_{\text{KL}}[q(\mathbf{x}_{0:T}), p_\theta(\mathbf{x}_{0:T})] \right), \quad (9)$$

The inequality $\mathcal{E} \geq 0$ always holds since KL divergence is non-negative.

3.3 LIMITED APPROXIMATION THEOREMS

In this part, we prove that the above defined errors are unbounded for current diffusion models. It's also worth noting that these errors already over-estimate the performances of diffusion models, since their definitions involve an infimum operation $\inf_{\theta \in \Theta}$.

Theorem 3.1 (Uniformly Unbounded Denoising Error). *For the diffusion process defined in Eq. 1 and the Gaussian denoising process defined in Eq. (2), given arbitrary real number N , there always exists a continuous data distribution $q(\mathbf{x}_0)$ (more specifically, Gaussian mixture) such that the inequality $\mathcal{M}_t > N$ holds for every denoising iteration $t \in [1, T]$.*

Remark 3.2. Uniform unboundedness is a very strict property, which requires the denoising error \mathcal{M}_t to be unbounded at every iteration t . In the case of ordinary unboundedness, the error \mathcal{M}_t might be unbounded for certain iterations but remain bounded for others.

Proof. We provide a complete proof to this theorem in the appendix. □

The above theorem not only implies that current diffusion models will fail to fit some complex data distribution $q(\mathbf{x}_t)$ because of its limited expressiveness in local denoising, but also indicates that the assumption of *perfect score functions* (i.e., bounded denoising errors) made by existing theoretical guarantees (Lee et al., 2022a; Chen et al., 2023) (which aims to prove that diffusion models are a universal approximator) are too strong.

Takeaway: The denoising error \mathcal{M}_t of current diffusion models can be arbitrarily large at every backward iteration $t \in [1, T]$, indicating that the assumption of *perfect score functions* made by existing theoretical guarantees is too strong.

Based on Theorem 3.1 and Proposition 3.1, we finally show that the global approximation error \mathcal{E} of current diffusion models is also unbounded.

Theorem 3.2 (Unbounded Approximation Error). *For the forward and backward processes respectively defined in Eq. (1) and Eq. (2), given any real number N , there always exists a continuous data distribution $q(\mathbf{x}_0)$ (specifically, Gaussian mixture) such that $\mathcal{E} > N$.*

Proof. A complete proof to this theorem is offered in the appendix. □

Since the negative likelihood $\mathbb{E}[-\log p_\theta(\mathbf{x}_0)]$ is computationally feasible, current practices (e.g., DDPM (Ho et al., 2020) and SGM Song et al. (2021b)) optimize the diffusion models by matching the backward process $p_\theta(\mathbf{x}_{0:T})$ with the forward process $q(\mathbf{x}_{0:T})$. This theorem indicates that this optimization scheme will fail for some complex data distribution $q(\mathbf{x}_0)$.

Takeaway: Under the current optimization scheme, diffusion models with simple Gaussian denoising $p_\theta(\mathbf{x}_{t-1} | \mathbf{x}_t) = \mathcal{N}(\mathbf{x}_{t-1}; \boldsymbol{\mu}_\theta(\mathbf{x}_t, t), \sigma_t \mathbf{I})$ will fail to well approximate some complex data distribution $q(\mathbf{x}_0)$ (e.g., Gaussian mixture).

4 METHOD: SOFT MIXTURE DENOISING

In light of our theoretical studies, we can see that current diffusion models are of limited expressiveness to approximate some complex data distribution $q(\mathbf{x}_0)$. To break this bottleneck, we introduce a new paradigm, **soft mixture denoising** (SMD), which permits the learnable backward module $p_\theta(\mathbf{x}_{t-1} | \mathbf{x}_t)$ to well fit non-Gaussian distribution $q(\mathbf{x}_{t-1} | \mathbf{x}_t)$. Not only does SMD have a solid theoretical foundation, but also it’s simple and efficient for implementation.

4.1 MAIN THEORY

Our theoretical analysis indicates that the *expressive bottleneck* of current diffusion models is mainly caused by the limited approximation capability of simple Gaussian denoising. Based on Proposition 3.1, an obvious way to address this problem is to directly model the backward probability $p_\theta(\mathbf{x}_{t-1} | \mathbf{x}_t)$ as a Gaussian mixture. For example, we have

$$p_\theta^{\text{mixture}}(\mathbf{x}_{t-1} | \mathbf{x}_t) = \sum_{k=1}^K z_{\theta_k}(\mathbf{x}_t, t) \mathcal{N}(\mathbf{x}_{t-1}; \boldsymbol{\mu}_{\theta_k}(\mathbf{x}_t, t), \boldsymbol{\Sigma}_{\theta_k}(\mathbf{x}_t, t)), \quad (10)$$

where $\theta = \{\theta_k | k \in [1, K] \cap \mathbb{N}^+\}$, the number of Gaussian components K is a hyper-parameter and weight $z_t^k(\cdot)$, mean $\boldsymbol{\mu}_{\theta_k}^k(\cdot)$, and covariance $\boldsymbol{\Sigma}_{\theta_k}^k(\cdot)$ that determine each component are all learnable. While the mixture model might be complex enough for backward denoising, it is not practical for two reasons: 1) it’s intractable to determine the number of components K from observed data; 2) mixture models are notoriously hard to optimize. Actually, Jin et al. (2016) proved that a Gaussian mixture model might be optimized into an arbitrarily bad local optimum.

Our method. To efficiently improve the expressiveness of diffusion models, we introduce *soft mixture denoising* (SMD) $p_\theta^{\text{SMD}}(\mathbf{x}_{t-1} | \mathbf{x}_t)$, a soft version of the mixture model $p_{\text{mixture}}(\cdot)$, which avoids specifying the number of mixture components K and permits effective optimization. Specifically, we define a continuous latent variable \mathbf{z}_t , as an alternative to mixture weight z_t^k , that represents the potential mixture structure of posterior distribution $q(\mathbf{x}_{t-1} | \mathbf{x}_t)$. Under this scheme, we model the learnable backward probability $p_\theta(\mathbf{x}_{t-1} | \mathbf{x}_t)$ as

$$p_\theta^{\text{SMD}}(\cdot) = \int_{\mathbf{z}_t} p_\theta^{\text{SMD}}(\mathbf{x}_{t-1}, \mathbf{z}_t | \mathbf{x}_t) d\mathbf{z}_t = \int_{\mathbf{z}_t} p_\theta^{\text{SMD}}(\mathbf{z}_t | \mathbf{x}_t) p_\theta^{\text{SMD}}(\mathbf{x}_{t-1} | \mathbf{x}_t, \mathbf{z}_t) d\mathbf{z}_t, \quad (11)$$

where $p_\theta(\mathbf{x}_{t-1} | \mathbf{x}_t, \mathbf{z}_t)$ is a learnable multivariate Gaussian:

$$p_\theta^{\text{SMD}}(\mathbf{x}_{t-1} | \mathbf{x}_t, \mathbf{z}_t) = \mathcal{N}(\mathbf{x}_{t-1}; \boldsymbol{\mu}_{\bar{\theta}, \tilde{\theta}(\mathbf{z}_t, t, \phi)}(\mathbf{x}_t, t), \boldsymbol{\Sigma}_{\bar{\theta}, \tilde{\theta}(\mathbf{z}_t, t, \phi)}(\mathbf{x}_t, t)). \quad (12)$$

Here both $\bar{\theta} \subset \theta$ and $\tilde{\theta}(\mathbf{z}_t, t, \phi), \phi \subset \theta$ constitute the parameter set of mean and covariance functions $\boldsymbol{\mu}_*, \boldsymbol{\Sigma}_*$. The latter differs from the former in its external dependencies on latent variable \mathbf{z}_t and iteration t . As a result, different values of the variable \mathbf{z}_t correspond to different parameterized Gaussians. This type of design is similar to the hypernetwork (Ha et al., 2017; Krueger et al., 2018). For implementation, we follow Eq. (2) to fix the covariance matrix $\boldsymbol{\Sigma}_*$ as $\sigma_t \mathbf{I}$ and adopt a similar parameterization of mean $\boldsymbol{\mu}_*(\mathbf{x}_t, t)$ as Eq. (4):

$$\boldsymbol{\mu}_{\bar{\theta}, \tilde{\theta}(\mathbf{z}_t, t, \phi)}(\mathbf{x}_t, t) = \frac{1}{\sqrt{\alpha_t}} \left(\mathbf{x}_t - \frac{\beta_t}{\sqrt{1 - \alpha_t}} \boldsymbol{\epsilon}_{\bar{\theta}, \tilde{\theta}(\mathbf{z}_t, t, \phi)}(\mathbf{x}_t, t) \right), \quad (13)$$

where $\boldsymbol{\epsilon}_*$ is a neural network. For image data, we build it as a U-Net (Ronneberger et al., 2015) (i.e., $\bar{\theta}$) with several extra layers that are computed from $\tilde{\theta}(\mathbf{z}_t, t, \phi)$.

Algorithm 1 Training

```

1: repeat
2:    $\mathbf{x}_0 \sim q(\mathbf{x}_0)$ 
3:    $t \sim \mathcal{U}\{1, T\}, \epsilon \sim \mathcal{N}(\mathbf{0}, \mathbf{I})$ 
4:    $\mathbf{x}_t = \sqrt{\alpha_t} \mathbf{x}_0 + \sqrt{1 - \alpha_t} \epsilon$ 
5:    $\mathbf{z}_t = g_\varphi(\boldsymbol{\eta}, \mathbf{x}_t, t), \boldsymbol{\eta} \sim \mathcal{N}(\mathbf{0}, \mathbf{I})$ 
6:    $\hat{\theta} = \{\bar{\theta}, \tilde{\theta}(\mathbf{z}_t, t, \phi)\}$ 
7:    $\theta = \{\bar{\theta}, \phi, \varphi\}$ 
8:   Update  $\theta$  w.r.t.  $\nabla_\theta \|\epsilon - \epsilon_{\hat{\theta}}(\mathbf{x}_t, t)\|^2$ 
9: until converged

```

Algorithm 2 Sampling

```

1:  $\mathbf{x}_T \sim p(\mathbf{x}_T) = \mathcal{N}(\mathbf{0}, \mathbf{I})$ 
2: for  $t = T, \dots, 1$  do
3:    $\epsilon \sim \mathcal{N}(\mathbf{0}, \mathbf{I})$  if  $t > 1$ , else  $\epsilon = 0$ 
4:    $\mathbf{z}_t = g_\varphi(\boldsymbol{\eta}, \mathbf{x}_t, t), \boldsymbol{\eta} \sim \mathcal{N}(\mathbf{0}, \mathbf{I})$ 
5:    $\hat{\theta} = \{\bar{\theta}, \tilde{\theta}(\mathbf{z}_t, t, \phi)\}$ 
6:    $\mathbf{x}_{t-1} = \frac{1}{\sqrt{\alpha_t}} \left( \mathbf{x}_t - \frac{1 - \alpha_t}{\sqrt{1 - \alpha_t}} \epsilon_{\hat{\theta}}(\mathbf{x}_t, t) \right) + \sigma_t \epsilon$ 
7: end for
8: return  $\mathbf{x}_0$ 

```

For the mixture component $p_\theta(\mathbf{z}_t | \mathbf{x}_t)$, we specify it as an arbitrarily complex distribution, which adds great flexibility into the learnable backward probability $p_\theta^{\text{SMD}}(\mathbf{x}_{t-1} | \mathbf{x}_t)$. For implementation, we adopt another neural network $g_\varphi : (\boldsymbol{\eta}, \mathbf{x}_t, t) \mapsto \mathbf{z}_t, \varphi \subset \theta$ with $\boldsymbol{\eta} \stackrel{\text{i.i.d.}}{\sim} \mathcal{N}(\mathbf{0}, \mathbf{I})$, which converts a standard Gaussian into a non-Gaussian distribution.

Theoretical guarantee. In the following, we prove that SMD $p_\theta^{\text{SMD}}(\mathbf{x}_{t-1} | \mathbf{x}_t)$ improves the expressiveness of diffusion models in fitting complex data distribution $q(\mathbf{x}_0)$.

Theorem 4.1 (Expressive Soft Mixture Denoising). *For the diffusion process defined in Eq. (1), suppose soft mixture model $p_\theta^{\text{SMD}}(\mathbf{x}_{t-1} | \mathbf{x}_t)$ is applied for backward denoising and data distribution $q(\mathbf{x}_0)$ is a Gaussian mixture, then both $\mathcal{M}_t = 0, \forall t \in [1, T]$ and $\mathcal{E} = 0$ hold.*

Remark 4.1. This conclusion should be compared with Theorems 3.1 and 3.2, which show vanilla diffusion models with simple Gaussian denoising might perform arbitrarily poorly in fitting some complex data distribution $q(\mathbf{x}_0)$ (e.g., Gaussian mixture).

Remark 4.2. The Gaussian mixture is a universal approximator for continuous probability distributions (Dalal & Hall, 1983). Therefore, this theorem implies that our proposed SMD permits the diffusion models to well approximate arbitrarily complex data distributions.

Proof. The proof to this theorem is fully provided in the appendix. \square

The implications of Theorem 3.1 and the above theorem are reflected in Fig. 1. With few backward iterations T , the posterior probability $q(\mathbf{x}_{t-1} | \mathbf{x}_t)$ will deviate much from a simple Gaussian. While vanilla diffusion models show poor performances in that case (as explained in Theorem 3.1), the models with SMD perform still well (as anticipated in Theorem 4.1).

4.2 EFFICIENT OPTIMIZATION AND SAMPLING

While Theorem 4.1 shows that SMD are highly expressive, it ideally assumes that neural networks are globally optimized. Plus, the latent variable in SMD introduces more complexity to the computation and analysis of diffusion models. To fully exploit the potential of SMD, it is important to develop efficient optimization and sampling algorithms.

Loss function. The negative log-likelihood for a diffusion model with the backward probability $p_\theta^{\text{SMD}}(\mathbf{x}_{t-1} | \mathbf{x}_t)$ of a latent variable model is formally defined as

$$\mathbb{E}_q[-\ln p_\theta^{\text{SMD}}(\mathbf{x}_0)] = \mathbb{E}_{\mathbf{x}_0 \sim q(\mathbf{x}_0)} \left[-\ln \left(\int_{\mathbf{x}_{1:T}} p(\mathbf{x}_T) \prod_{t=T}^1 p_\theta^{\text{SMD}}(\mathbf{x}_{t-1} | \mathbf{x}_t) d\mathbf{x}_{1:T} \right) \right]. \quad (14)$$

Like vanilla diffusion models, this log-likelihood term is also computationally infeasible. In the following, we derive its upper bound for optimization.

Proposition 4.1 (Upper Bound of Negative Log-likelihood). *Suppose the diffusion process is defined as Eq. (1) and the soft mixture model $p_\theta^{\text{SMD}}(\mathbf{x}_{t-1} | \mathbf{x}_t)$ is applied for backward denoising, then an*

Dataset / Model	DDPM	DDPM w/ SMD	ADM	ADM w/ SMD
CIFAR-10 (32 × 32)	3.78	3.13	2.98	2.55
LSUN-Conference (64 × 64)	4.15	3.52	3.85	3.29
LSUN-Church (64 × 64)	3.65	3.17	3.41	2.98
CelebA-HQ (128 × 128)	6.78	6.35	6.45	6.02

Table 1: The FID scores of our models and the baselines on common image datasets. We set $T = 1000$ for all models and apply that number of iterations for stochastic sampling.

upper bound of the expected negative log-likelihood $\mathbb{E}_q[-\ln p_{\theta}^{\text{SMD}}(\mathbf{x}_0)]$ is

$$\mathcal{L}^{\text{SMD}} = C + \sum_{t=1}^T \mathbb{E}_{\boldsymbol{\eta}, \boldsymbol{\epsilon}, \mathbf{x}_0} \left[\Gamma_t \|\boldsymbol{\epsilon} - \boldsymbol{\epsilon}_{\tilde{\theta}, \tilde{g}_{\varphi}(\cdot), t, \phi}(\sqrt{\bar{\alpha}_t} \mathbf{x}_0 + \sqrt{1 - \bar{\alpha}_t} \boldsymbol{\epsilon}, t)\|^2 \right], \quad (15)$$

where $g_{\varphi}(\cdot) = g_{\varphi}(\boldsymbol{\eta}, \sqrt{\bar{\alpha}_t} \mathbf{x}_0 + \sqrt{1 - \bar{\alpha}_t} \boldsymbol{\epsilon}, t)$, C is a constant that does not involve any model parameter $\theta = \tilde{\theta} \cup \phi \cup \varphi$, $\mathbf{x}_0 \sim q(\mathbf{x}_0)$, $\boldsymbol{\eta}, \boldsymbol{\epsilon}$ are two independent Gaussian noises drawn from $\mathcal{N}(\mathbf{0}, \mathbf{I})$, and $\Gamma_t = \beta_t^2 / (2\sigma_t \alpha_t (1 - \bar{\alpha}_t))$.

Proof. The detailed derivation to get the upper bound \mathcal{L}^{SMD} is in the appendix. \square

Compared with the loss function of vanilla diffusion models (i.e., Eq. (5)), our upper bound mainly differs in the hypernetwork $\tilde{\theta}$ to parameterize the denoising function $\boldsymbol{\epsilon}_*$ and an expectation operation $\mathbb{E}_{\boldsymbol{\eta}}$. The former is computed by neural networks and the latter is approximated by Monte Carlo sampling, which both add minor computational costs.

Training and Inference. Our training and sampling procedures are also distinct from those of vanilla diffusion models. Their details are in Algorithm 1 and Algorithm 2, with blue lines to show where our diffusion model is distinct from the vanilla model.

For the training procedure, we follow the common practices (Ho et al., 2020; Dhariwal & Nichol, 2021) to apply Monte Carlo sampling to handle iterated expectations $\mathbb{E}_{\boldsymbol{\eta}, \boldsymbol{\epsilon}, \mathbf{x}_0}$ in Eq. (15) and reweight loss term $\|\boldsymbol{\epsilon} - \boldsymbol{\epsilon}_*(\mathbf{x}_t, t)\|^2$ by ignoring coefficient Γ_t . One might also sample more noises (e.g., $\boldsymbol{\eta}$) in one training step to trade run-time efficiency for approximation accuracy.

For the sampling procedure, we simply compute the latent variable \mathbf{z}_t through drawing a sample from its source distribution $\mathcal{N}(\mathbf{0}, \mathbf{I})$ and feed the sample into the non-linear mapping g_{φ} . In fact, one can resort to normalizing flow (Kingma & Dhariwal, 2018) to build a invertible mapping g_{φ} such that the operation $\max_{\mathbf{z}_t} p_{\theta}^{\text{SMD}}(\mathbf{z}_t \mid \mathbf{x}_t)$ is computationally feasible. In that way, we might better estimate the latent variable \mathbf{z}_t . However, our current implementation is more efficient and we find it empirically performs well in practice.

5 EXPERIMENTS

To verify the effectiveness of our proposed SMD, we have performed extensive experiments on multiple image datasets. Firstly, we show that SMD significantly improves different types of diffusion models (e.g., LDM) on all datasets. Then, we demonstrate that SMD makes the diffusion models robust to few backward iterations. Lastly, we try sampling more than one $\boldsymbol{\eta}$ for loss estimation, which further improves the performance but causes an extra time cost.

5.1 RESULTS ON IMAGE DATASETS

We select 3 most common baselines and 4 image datasets to show how our proposed SMD quantitatively improves diffusion models. The baselines include DDPM Ho et al. (2020), ADM (Dhariwal & Nichol, 2021), and Latent Diffusion Model (LDM) (Pinaya et al., 2022). The datasets include CIFAR-10 (Krizhevsky et al., 2009), LSUN-Conference, LSUN-Church (Yu et al., 2015), and CelebA-HQ (Liu et al., 2015). For all models, we set the backward iterations T as 1000 and stochastically sample 10000 images for computing the FID scores.

Model / Dataset	LSUN-Church (256 × 256)	CelebA-HQ (256 × 256)
LDM	5.86	6.13
LDM w/ SMD	5.21	5.48

Table 2: The FID scores of our model and the baseline on high-resolution image datasets. We set $T = 1000$ for all models and apply that number of iterations for stochastic sampling.

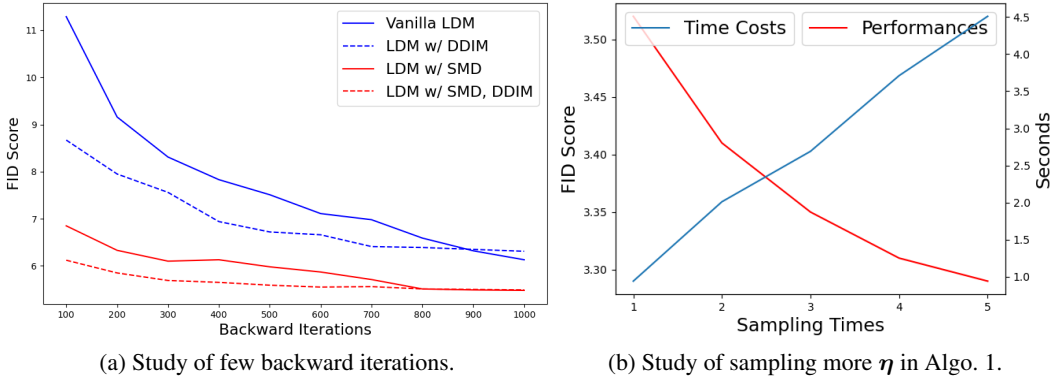


Figure 2: The left study is conducted on CelebA-HQ (256 × 256) and the right one is performed on LSUN-Conference (64 × 64) with DDPM w/ SMD.

We divide the experiment results into two subsets in terms of image resolutions. One part is the results on the image datasets of low and middle resolutions. As shown in Table 1, our proposed SMD significantly improves both DDPM and ADM on all datasets. For example, our models outperform DDPM by 15.14% on LSUN-Church and ADM by 16.86%. The other part is the results on high-resolution image datasets. We adopt LDM as the baseline since it eats much less memory as other diffusion models (e.g., DDPM). As shown in Table 2, SMD notably decreases the FID scores of LDM by 12.47% on LSUN-Church and 11.86% on CelebA-HQ. All these results strongly verify that SMD is highly effective in improving the performances of diffusion models.

5.2 FEW BACKWARD ITERATIONS

Intuitively, in the situation of few denoising iterations, the posterior forward probability $q(\mathbf{x}_{t-1} | \mathbf{x}_t)$ will greatly drift from a simple Gaussian, which is hard for the learnable backward probability $p_\theta(\mathbf{x}_{t-1} | \mathbf{x}_t)$ to approximate. Based on Theorems 3.2 and 4.1, we can anticipate that our models will be more robust to this effect than vanilla diffusion models.

The solid blue and red curves in Fig. 2a respectively show how the F1 scores of vanilla LDM and LDM w/ SMD change with respect to increasing backward iterations. We can see that our proposed SMD improves the LDM much more at fewer backward iterations (e.g., $T = 200$), which is line with our expectation. Besides, we also apply DDIM (Song et al., 2021a), a popular fast sampler, to our model and the baseline. We can see that the performances of both models are generally improved because of the deterministic sampling.

5.3 LATENT VARIABLE SAMPLING

In Algorithm 1, we only sample one η at a time for maintaining high computational efficiency. Actually, we can sample more to estimate the loss better. Fig 2b shows how the time cost of one training step and the FID score of our model change in terms of the sampling times of noise η . While the time cost linearly goes up with the increasing sampling times, the FID score of our model gradually decreases and has a trend to converge.

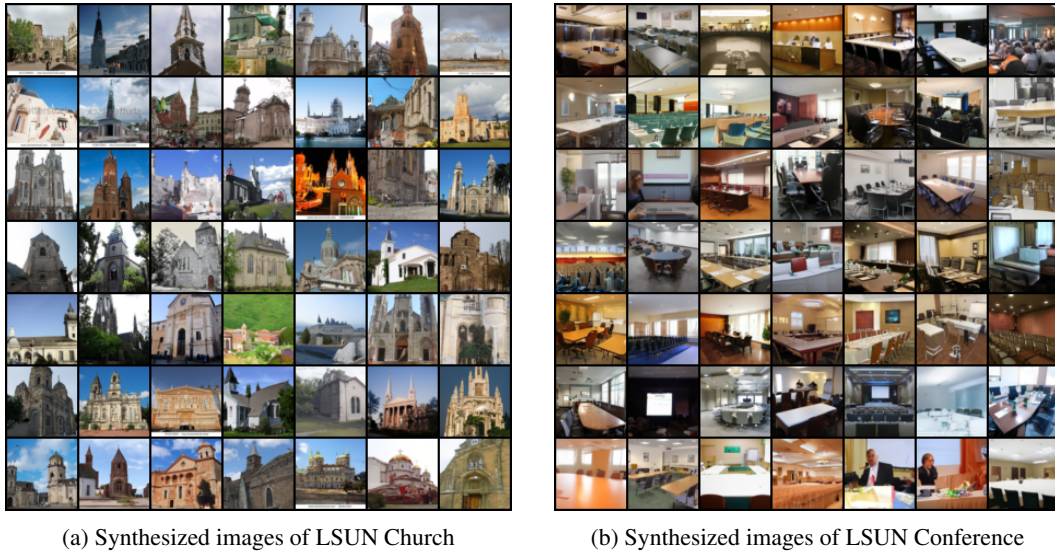


Figure 3: 64×64 images generated by DDPM w/ SMD.



Figure 4: Generated images on CelebA-HQ 128×128 (left) and 256×256 (right). The left samples are from DDPM w/ SMD and the right ones from LDM w/ SMD.

A PROOFS

The proofs to our propositions and theorems are all done and will be publicly available in arXiv once the paper is accepted.

B GENERATED SAMPLES

Some images generated by our models (e.g., LDM w/ SMD) are in Fig. 3 and Fig. 4.

REFERENCES

Peter Ahrendt. The multivariate gaussian probability distribution. *Technical University of Denmark, Tech. Rep*, pp. 203, 2005.

- Sitan Chen, Sinho Chewi, Jerry Li, Yuanzhi Li, Adil Salim, and Anru Zhang. Sampling is as easy as learning the score: theory for diffusion models with minimal data assumptions. In *The Eleventh International Conference on Learning Representations*, 2023. URL https://openreview.net/forum?id=zyLVMgsZ0U_.
- SR Dalal and WJ Hall. Approximating priors by mixtures of natural conjugate priors. *Journal of the Royal Statistical Society: Series B (Methodological)*, 45(2):278–286, 1983.
- Pieter-Tjerk De Boer, Dirk P Kroese, Shie Mannor, and Reuven Y Rubinstein. A tutorial on the cross-entropy method. *Annals of operations research*, 134:19–67, 2005.
- Prafulla Dhariwal and Alexander Nichol. Diffusion models beat gans on image synthesis. In M. Ranzato, A. Beygelzimer, Y. Dauphin, P.S. Liang, and J. Wortman Vaughan (eds.), *Advances in Neural Information Processing Systems*, volume 34, pp. 8780–8794. Curran Associates, Inc., 2021. URL <https://proceedings.neurips.cc/paper/2021/file/49ad23d1ec9fa4bd8d77d02681df5cfa-Paper.pdf>.
- Ian Goodfellow, Jean Pouget-Abadie, Mehdi Mirza, Bing Xu, David Warde-Farley, Sherjil Ozair, Aaron Courville, and Yoshua Bengio. Generative adversarial nets. In Z. Ghahramani, M. Welling, C. Cortes, N. Lawrence, and K.Q. Weinberger (eds.), *Advances in Neural Information Processing Systems*, volume 27. Curran Associates, Inc., 2014. URL <https://proceedings.neurips.cc/paper/2014/file/5ca3e9b122f61f8f06494c97b1afccf3-Paper.pdf>.
- Ian Goodfellow, Yoshua Bengio, and Aaron Courville. *Deep learning*. MIT press, 2016.
- David Ha, Andrew M. Dai, and Quoc V. Le. Hypernetworks. In *International Conference on Learning Representations*, 2017. URL <https://openreview.net/forum?id=rkpACellx>.
- Jonathan Ho, Ajay Jain, and Pieter Abbeel. Denoising diffusion probabilistic models. *Advances in Neural Information Processing Systems*, 33:6840–6851, 2020.
- Marco F Huber, Tim Bailey, Hugh Durrant-Whyte, and Uwe D Hanebeck. On entropy approximation for gaussian mixture random vectors. In *2008 IEEE International Conference on Multisensor Fusion and Integration for Intelligent Systems*, pp. 181–188. IEEE, 2008.
- Chi Jin, Yuchen Zhang, Sivaraman Balakrishnan, Martin J Wainwright, and Michael I Jordan. Local maxima in the likelihood of gaussian mixture models: Structural results and algorithmic consequences. *Advances in neural information processing systems*, 29, 2016.
- Durk P Kingma and Prafulla Dhariwal. Glow: Generative flow with invertible 1x1 convolutions. In S. Bengio, H. Wallach, H. Larochelle, K. Grauman, N. Cesa-Bianchi, and R. Garnett (eds.), *Advances in Neural Information Processing Systems*, volume 31. Curran Associates, Inc., 2018. URL <https://proceedings.neurips.cc/paper/2018/file/d139db6a236200b21cc7f752979132d0-Paper.pdf>.
- Zhifeng Kong, Wei Ping, Jiaji Huang, Kexin Zhao, and Bryan Catanzaro. Diffwave: A versatile diffusion model for audio synthesis. In *International Conference on Learning Representations*, 2021. URL <https://openreview.net/forum?id=a-xFK8Ymz5J>.
- Alex Krizhevsky, Geoffrey Hinton, et al. Learning multiple layers of features from tiny images. 2009.
- David Krueger, Chin-Wei Huang, Riashat Islam, Ryan Turner, Alexandre Lacoste, and Aaron Courville. Bayesian hypernetworks, 2018. URL <https://openreview.net/forum?id=S1fcY-Z0->.
- Holden Lee, Jianfeng Lu, and Yixin Tan. Convergence of score-based generative modeling for general data distributions. In *NeurIPS 2022 Workshop on Score-Based Methods*, 2022a. URL <https://openreview.net/forum?id=Sg19A8mu8sv>.
- Holden Lee, Jianfeng Lu, and Yixin Tan. Convergence for score-based generative modeling with polynomial complexity. *Advances in Neural Information Processing Systems*, 35:22870–22882, 2022b.

- Xiang Lisa Li, John Thickstun, Ishaan Gulrajani, Percy Liang, and Tatsunori Hashimoto. Diffusion-LM improves controllable text generation. In Alice H. Oh, Alekh Agarwal, Danielle Belgrave, and Kyunghyun Cho (eds.), *Advances in Neural Information Processing Systems*, 2022. URL <https://openreview.net/forum?id=3s9IrEsjLyk>.
- Ziwei Liu, Ping Luo, Xiaogang Wang, and Xiaoou Tang. Deep learning face attributes in the wild. In *Proceedings of International Conference on Computer Vision (ICCV)*, December 2015.
- Cheng Lu, Yuhao Zhou, Fan Bao, Jianfei Chen, Chongxuan Li, and Jun Zhu. Dpm-solver: A fast ode solver for diffusion probabilistic model sampling in around 10 steps. *Advances in Neural Information Processing Systems*, 35:5775–5787, 2022.
- Walter HL Pinaya, Petru-Daniel Tudosiu, Jessica Dafflon, Pedro F Da Costa, Virginia Fernandez, Parashkev Nachev, Sebastien Ourselin, and M Jorge Cardoso. Brain imaging generation with latent diffusion models. In *MICCAI Workshop on Deep Generative Models*, pp. 117–126. Springer, 2022.
- Danilo Rezende and Shakir Mohamed. Variational inference with normalizing flows. In Francis Bach and David Blei (eds.), *Proceedings of the 32nd International Conference on Machine Learning*, volume 37 of *Proceedings of Machine Learning Research*, pp. 1530–1538, Lille, France, 07–09 Jul 2015. PMLR. URL <https://proceedings.mlr.press/v37/rezende15.html>.
- Robin Rombach, Andreas Blattmann, Dominik Lorenz, Patrick Esser, and Björn Ommer. High-resolution image synthesis with latent diffusion models. In *Proceedings of the IEEE/CVF Conference on Computer Vision and Pattern Recognition*, pp. 10684–10695, 2022.
- Olaf Ronneberger, Philipp Fischer, and Thomas Brox. U-net: Convolutional networks for biomedical image segmentation. In *Medical Image Computing and Computer-Assisted Intervention—MICCAI 2015: 18th International Conference, Munich, Germany, October 5-9, 2015, Proceedings, Part III 18*, pp. 234–241. Springer, 2015.
- Peter J Rousseeuw and Annick M Leroy. *Robust regression and outlier detection*. John Wiley & sons, 2005.
- Claude Elwood Shannon. A mathematical theory of communication. *ACM SIGMOBILE mobile computing and communications review*, 5(1):3–55, 2001.
- Jascha Sohl-Dickstein, Eric Weiss, Niru Maheswaranathan, and Surya Ganguli. Deep unsupervised learning using nonequilibrium thermodynamics. In *International Conference on Machine Learning*, pp. 2256–2265. PMLR, 2015.
- Jiaming Song, Chenlin Meng, and Stefano Ermon. Denoising diffusion implicit models. In *International Conference on Learning Representations*, 2021a. URL <https://openreview.net/forum?id=StlgiaRCHLP>.
- Yang Song, Jascha Sohl-Dickstein, Diederik P Kingma, Abhishek Kumar, Stefano Ermon, and Ben Poole. Score-based generative modeling through stochastic differential equations. In *International Conference on Learning Representations*, 2021b. URL <https://openreview.net/forum?id=PXTIG12RRHS>.
- Fisher Yu, Ari Seff, Yinda Zhang, Shuran Song, Thomas Funkhouser, and Jianxiong Xiao. Lsun: Construction of a large-scale image dataset using deep learning with humans in the loop. *arXiv preprint arXiv:1506.03365*, 2015.
- Yufeng Zhang, Wanwei Liu, Zhenbang Chen, Kenli Li, and Ji Wang. On the properties of kullback-leibler divergence between gaussians. *arXiv preprint arXiv:2102.05485*, 2021.